Plasma-assisted nitrogen fixation: the effect of water presence

Mikhail Gromov[a,b,*] and Nefeli Kamarinopoulou[c,d], Nathalie De Geyter[b], Rino Morent[b], Rony Snyders[a,e], Dionisios Vlachos[c,d], Panagiotis Dimitrakellis[c,d], and Anton Nikiforov[b]

[a.] *Chimie des Interactions Plasma-Surface (ChIPS), CIRMAP, Mons University, 7000-Mons, Belgium.*
[b.] *Research Unit Plasma Technology (RUPT), Department of Applied Physics, Ghent University, 9000-Gent, Belgium.*
[c.] *Department of Chemical and Biomolecular Engineering, University of Delaware, Newark, Delaware 19716, United States.*
[d.] *Catalysis Center for Energy Innovation, University of Delaware, Newark, Delaware 19716, United States.*
[e.] *Materia Nova Research Centre, Parc Initialis, 7000-Mons, Belgium.*
** Author to whom correspondence should be addressed: mikhail.gromov@ugent.be*

Equivalent electrical scheme and resistivity calculations

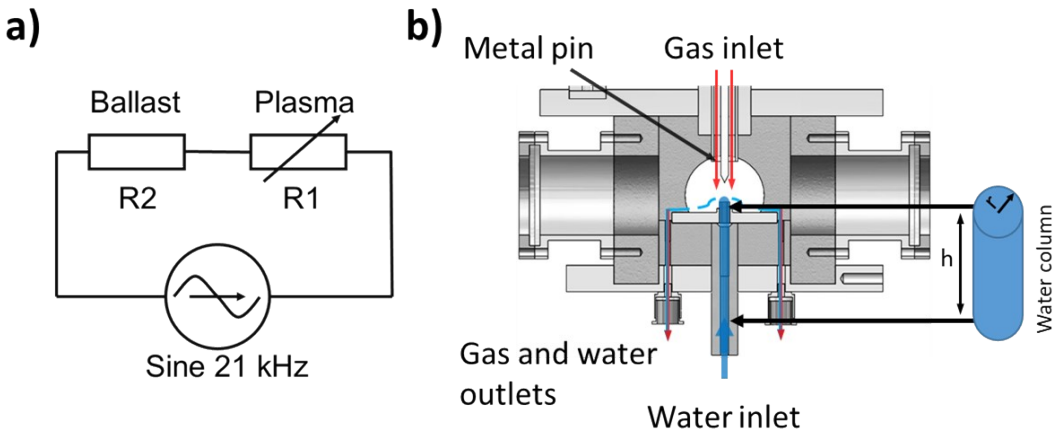

FIG. S1. (a) Equivalent scheme of the plasma systems; (b) pin-to-liquid system with denoting water column geometry used to calculate resistivity.

Figure S1a shows the equivalent electrical scheme of the plasma systems in pin-to-pin (PP) and pin-to-liquid (PL) configurations where $R1$ and $R2$ denote a variable resistivity of the discharge gap and a ballast that restricts the current, respectively. In the case of the PL discharge, the water column between the ground connection and the plasma/liquid interface shown in Figure S1b is considered as the ballast ($R2$) and was estimated as follows:

$$R_2^{PL} = \rho \cdot \frac{h}{\pi r^2}, \rho = \frac{1}{550 \cdot 10^{-6}} (\Omega \cdot cm); h = 1.1\ (cm); r = 0.115\ (cm)$$

where ρ is the resistivity of the medium, h is the height of the water column, and r is the radius of the water channel. In the PP configuration, a 50 kΩ resistor ($R2$) was used to create two similar plasmas.

Optical emission spectroscopy (OES)

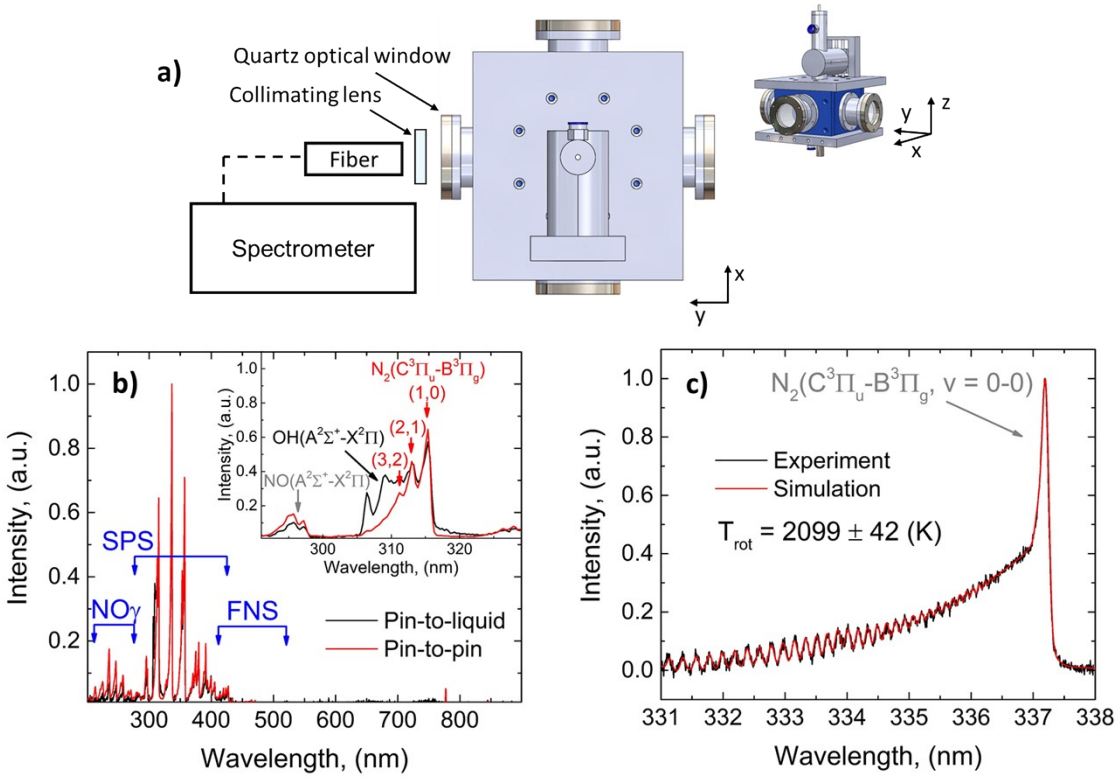

FIG. S2. (a) Schematic representation of the optical emission collection system. (b) Wide-range optical emission spectra taken at a power of 12 W measured using an Ocean Optics S2000 spectrometer (SPS – second positive system of N_2; FNS – first negative system of N_2). (c) An example of the fitted spectrum using massiveOES software in pin-to-pin setup configuration using a power of 4 W.

Ion chromatography: analysis and calibration procedures

Nitrites ($^{NO_2^-}$) and nitrates ($^{NO_3^-}$) in the liquid phase were measured with a Metrohm 940 ProfIC Vario 14 ion chromatograph equipped with a Metrosep A Supp 5 column (4 x 100 mm), an MSMS-A Rotor suppressor, and a conductivity detector. The eluent was a solution of 3.2 mM Na_2CO_3 and 1 mM $NaHCO_3$ with a flow rate of 0.4 mL/min. The column conductivity was 3.71 µS/cm. The temperature was set at 30°C and the pressure at 3.72 MPa. The calibration curves for $^{NO_2^-}$ and $^{NO_3^-}$ species were made with standard solutions of $NaNO_2$ (Sigma Aldrich ≥97%) and $NaNO_3$ (Sigma Aldrich ≥99%), respectively. The retention time for $^{NO_2^-}$ and $^{NO_3^-}$ species was ~8.1 min and 11.1 min, respectively. To ensure accurate quantification of $^{NO_2^-}$ species, the calibration curves were obtained for low and high concentration ranges, as shown in Figures S2a and S2b. $^{NO_3^-}$ quantification was performed according to the calibration curve presented in Figure S2c.

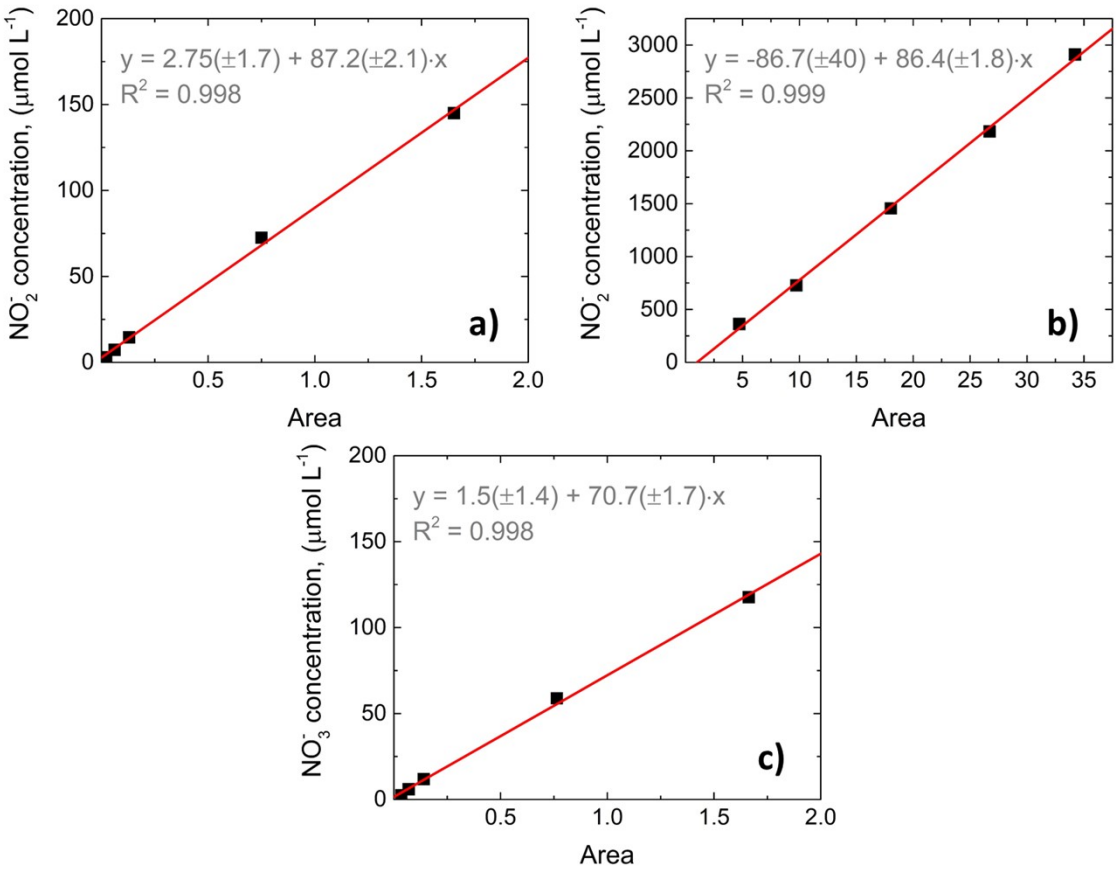

FIG. S3. Calibration curves for ion chromatography: (a) NO_2^- in the lower concentration range of 2.9 µM ≤ [NO_2^-] ≤ 0.14 mM, (b) NO_2^- in the higher concentration range of 0.14 mM < [NO_2^-] ≤ 2.9 mM, (c) NO_3^- in the concentration range of 2.35 µM ≤ [NO_3^-] ≤ 0.12 mM. The deviation interval of the measurements is < 1%.

Plasma visualization via a photomultiplier tube (PMT)

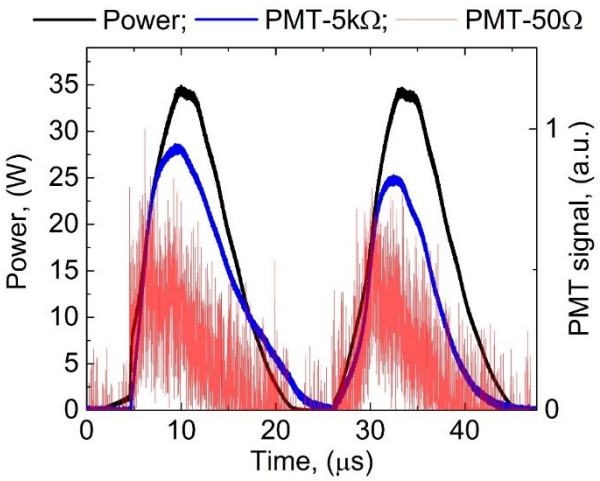

FIG. S4. Power waveform and PMT signals recorded with a time response of 5 ns (PMT-50Ω) and 500 ns (PMT-5kΩ).

The plasma temperatures at different gas flow rates

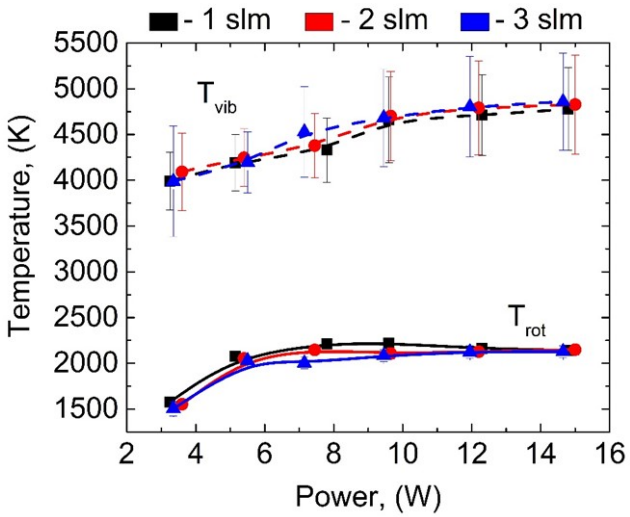

FIG. S5. Effect of the gas flow on the gas temperatures in the pin-to-pin system.

The energy efficiency of the N-fixation process

The production energy efficiency (EE) of component X in the gas phase was determined assuming linear behavior of the measured species with power as:

$$EE = \sum_X C_X \cdot 10^{-6} \cdot \frac{flow\ rate}{V_{molar}} \cdot M(X) \cdot \frac{1}{Power}\ [g \cdot kWh^{-1}],$$

where C is the concentration of component X (NO, NO_2, N_2O, HNO_2) in ppm, V_{molar} is the molar volume in $l\,mol^{-1}$, the gas flow is in $l\,h^{-1}$, M is the molar mass of component X in $g\,mol^{-1}$, and the $Power$ is expressed in kW.

The energy efficiency (EE) of NO_x^- in the liquid phase was obtained as follows:

$$EE = \sum_{X} C_{NO_x^-} \cdot 10^{-6} \cdot \frac{V \cdot \rho_{H_2O}}{M_{H_2O}} \cdot M_{NO_x^-} \cdot \frac{1}{t \cdot Power} [g \cdot kWh^{-1}],$$

where C is the concentration of component NO_x^- (NO_2^-, NO_3^-) in the liquid in ppm, V is the volume of the liquid in l, ρ_{H_2O} is water density in $g\,l^{-1}$, M is the molar mass in $g\,mol^{-1}$, and t is the treatment time in h.

The energy efficiencies averaged over the power range from 4 to 20 W are presented in FIG. 8. An example of an energy efficiency calculation is shown below for the PLb system using a gas flow rate of 1 slm. The rest of the experimental sets were used similarly to obtain the corresponding energy efficiencies.

Constants:

1slm	
Constants:	
Gas flow rate, l/h	60
Vmolar, l/mol	22.4
M(NO), g/mol	30
M(NO2), g/mol	46
M(NO3), g/mol	62
M(N2O), g/mol	44
M(HNO2), g/mol	47
Volume, l	0.5
Trin. Time, h	0.166667

Gas phase concentrations to EE:

PLb				
power, W	NO	NO2	N2O	HNO2
W	ppm	ppm	ppm	ppm
4.00	325.39	-12.55	4.41	16.39
4.84	363.91	21.68	4.48	36.71
5.68	402.43	55.91	4.55	57.03
6.53	440.96	90.14	4.62	77.35
7.37	479.48	124.37	4.69	97.67
8.21	518.00	158.60	4.76	118.00
9.05	556.53	192.83	4.84	138.32
9.89	595.05	227.06	4.91	158.64
10.74	633.58	261.29	4.98	178.96
11.58	672.10	295.52	5.05	199.28
12.42	710.62	329.75	5.12	219.60
13.26	749.15	363.98	5.20	239.92
14.11	787.67	398.21	5.27	260.24
14.95	826.20	432.44	5.34	280.56
15.79	864.72	466.67	5.41	300.88
16.63	903.24	500.90	5.48	321.20
17.47	941.77	535.13	5.56	341.52
18.32	980.29	569.36	5.63	361.84
19.16	1018.82	603.59	5.70	382.16
20.00	1057.34	637.82	5.77	402.48

power, W	NO	NO2	N2O	HNO2	NOX+HNO
W	g/kWh	g/kWh	g/kWh	g/kWh	g/kWh
4.00	6.54	-0.39	0.13	0.52	6.80
4.84	6.04	0.55	0.11	0.95	7.65
5.68	5.69	1.21	0.09	1.26	8.26
6.53	5.43	1.70	0.08	1.49	8.71
7.37	5.23	2.08	0.08	1.67	9.05
8.21	5.07	2.38	0.07	1.81	9.33
9.05	4.94	2.62	0.06	1.92	9.55
9.89	4.83	2.83	0.06	2.02	9.74
10.74	4.74	3.00	0.05	2.10	9.89
11.58	4.66	3.14	0.05	2.17	10.03
12.42	4.60	3.27	0.05	2.23	10.14
13.26	4.54	3.38	0.05	2.28	10.24
14.11	4.49	3.48	0.04	2.32	10.33
14.95	4.44	3.56	0.04	2.36	10.41
15.79	4.40	3.64	0.04	2.40	10.48
16.63	4.36	3.71	0.04	2.43	10.55
17.47	4.33	3.77	0.04	2.46	10.60
18.32	4.30	3.83	0.04	2.49	10.65
19.16	4.27	3.88	0.04	2.51	10.70
20.00	4.25	3.93	0.03	2.53	10.75
		EE in the gas phase [g/kWh]:			
			AVERAGE	AVEDEV	
			9.69	0.85	

Liquid phase concentrations to EE:

Power	NO2-	NO3-
W	ppm	ppm
4.00	0.20	0.13
4.84	0.97	0.26
5.68	1.74	0.39
6.53	2.51	0.52
7.37	3.27	0.65
8.21	4.04	0.78
9.05	4.81	0.90
9.89	5.58	1.03
10.74	6.34	1.16
11.58	7.11	1.29
12.42	7.88	1.42
13.26	8.64	1.55
14.11	9.41	1.68
14.95	10.18	1.81
15.79	10.95	1.94
16.63	11.71	2.06
17.47	12.48	2.19
18.32	13.25	2.32
19.16	14.02	2.45
20.00	14.78	2.58

Power	NO2-	NO3-
W	g/kWh	g/kWh
4.00	0.39	0.34
4.84	1.53	0.55
5.68	2.34	0.71
6.53	2.93	0.82
7.37	3.40	0.90
8.21	3.76	0.97
9.05	4.06	1.03
9.89	4.31	1.08
10.74	4.52	1.12
11.58	4.69	1.15
12.42	4.85	1.18
13.26	4.98	1.20
14.11	5.10	1.23
14.95	5.21	1.25
15.79	5.30	1.26
16.63	5.38	1.28
17.47	5.46	1.29
18.32	5.53	1.31
19.16	5.59	1.32
20.00	5.65	1.33

EE in the liquid phase [g/kWh]:

	AVERAGE	AVEDEV
	5.30	1.35

Negative concentrations indicate that the formation processes at low plasma power differ and do not follow the linear trend.